

# **Novel machine and measurement concept for micro machining by selective laser sintering**

Erler M, Streek A, Schulze C, Exner H.  
Laserinstitut Hochschule Mittweida, University of applied Science Mittweida  
Mittweida  
D-09648  
[erler2@hs-mittweida.de](mailto:erler2@hs-mittweida.de)

## **Keywords**

Laser micro sintering, micro powder, 3D-measurement, in-situ

REVIEWED

## **Abstract**

Laser sintering has been established in solid freeform fabrication to produce individual micro parts and small batches. However, the achievable resolution and accuracy of this technology seems to be not sufficient to meet prospective demands in micro production, i.e. micro system technology, aerospace or innovative medical applications. As a modification of the technology, laser micro sintering (LMS) was developed to overcome this limitation. In general, the results obtained in LMS demonstrated already the high potential of this additive manufacturing process in micro production. The limited dimensions of the micro parts and even the reproducibility, due to the special process requirements regarding the applied powder particles sizes in the  $\mu\text{m}$ -ranges, inhibits the implementation as an industrial manufacturing process. Therefore a novel concept of setups, suitable for an industrial demand of selective laser sintering with noticeable higher resolutions has to be proven. As a first, a novel machinery setup for a high resolution selective laser sintering has been studied in this work. To achieve a sufficient repeatability of the sintering process, a new method for in-situ analyzing and measuring is implemented and allows the verification the homogeneity and thickness first: of the deposited powder layers and second: of the resulting sinter structure. As an innovative feature the measurement system has to be applied as an in-situ method for direct process controlling in a future use. Accordingly, the possibility to recognize structural defects during generation of sintered bodies are presented and comparably analyzed by cross sections of the respective specimens.

## **Introduction**

Since 2002, the process of selective laser micro sintering is continuously developed by Laserinstitut Hochschule Mittweida (LHM). It is a modification of selective laser sintering to generate metal micro parts. The minimal achievable structural resolutions are  $30\ \mu\text{m}$  with sinter layer thickness down to  $1\ \mu\text{m}$ . For the manufacturing of high-resolution components, micro-powders were to be applied. Disadvantage of appliance micro powders compared to powders for the commercial sintering is the tendency to format agglomerates, a poor flowability and a low bulk density. These special properties results in a poor control of the powder coating and a limited reproducibility of manufacturing process. Therefore, the implementation as an industrial manufacturing process is inhibits. Additionally, a increasing of the build speed, from the current maximum  $35\ \text{mm}^3/\text{h}$  for a high resolution sinter part, becoming more and more industrial significance. Therefore, the resulting coating time is a

important factor to achieve a high build speed. The current coating system [Fig. 1] shows that defined and homogenous powder beds can only be achieved by a slow coating (4-6 s). By using higher coating speeds frequent powder layer defects occur, finally affecting the quality of the sintered layers [Fig. 1b]. Another factor of the build speed is the irradiation time. At the present, q-switched lasers with maximum output powers of 20 W and scanning-speeds of up to 2 m/s are used. Current fundamental research at LHM focused on the high rate micro sintering [3, 4]. By using high-power lasers and a polygon scanner irradiation times should be significantly reduced. Further optimization potential is the increasing of the sinter densities (current 60-70%). Investigations of a powder packing after the powder coating process has already shown that this sinter densities can be increased to 97% [1, 2]. However, the subsequent packing process reduces the build speed of the generating process, but showed the already high potential of a powder condensed sintering.

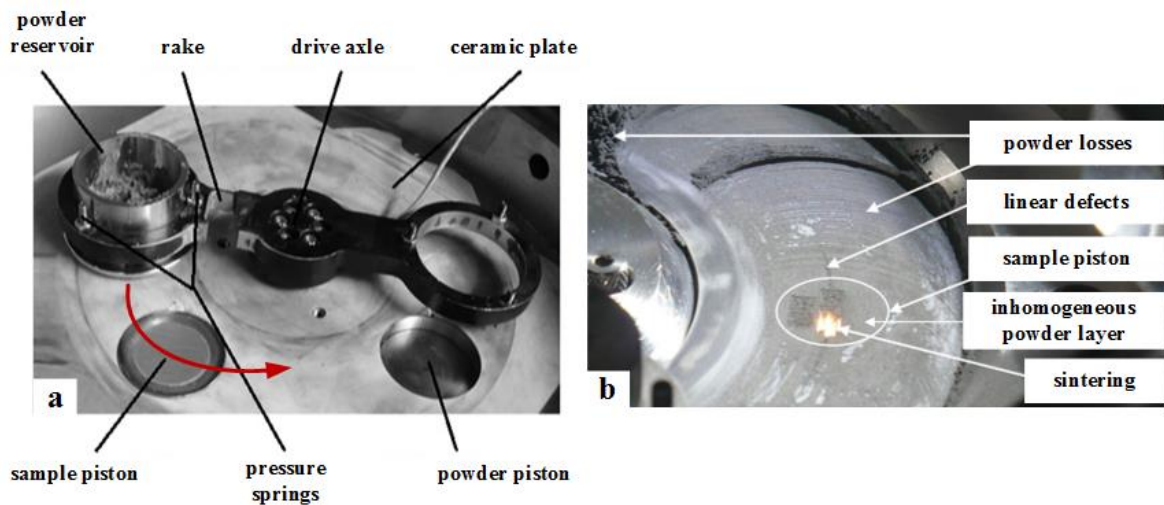


*Fig. 1: (a) The current coating system. The powder is transported by a ringrake from the powder piston to the sample piston. (b) Detailed view of the running sintering process shows some powder layer defects*

Summarizing, there is a necessity for a novel powder coating regime / device. The goal is to combine powder packing and powder coating with simultaneous reduction of the coating times. For the analysis of the powder layer and the resulting sinter layer regarding the homogeneity, thickness and layer defects, a 3D measurement system has to be integrated into the sinter system. Furthermore, correlations between the layer defects and the recorded measured data should be found to increase the reproducibility of the generating process.

### **General technique and equipment**

A 3D measuring system to evaluate and analyze the novel coating systems is required. Therefore, the integration of the 3D measuring system and experimental investigation are done in an existing setup for a high-rate laser microsintering [Fig. 1]. A single-mode CW Ytterbium fiber laser system YLR-400-SM-LP (IPG) was applied. The maximum laser output power was 400 W with a times-diffraction-limit-factor of  $M^2 < 1.5$ . The laser beam is switched via an acousto-optical modulator with a maximum frequency of 1 MHz and a minimal laser on time of 178 ns [5]. The deflection of the laser beam was realized by a high aperture galvanometer scanner (Scanlab: SS-LD-30) with a maximum scan of 12 m/s. For the experiments, an f-theta-objective with a focal length of 230 mm and a beam expander result in

a focal spot size of  $d_{86}=35\ \mu\text{m}$ . The sintered specimens were generated under environmental atmosphere. As measurement system a 2D laser displacement sensor made by Keyence (LJ-G030) was used, which operates according to the principle of optical triangulation (light section method). The spot diameter of the measuring laser line is  $40\ \mu\text{m} \times 25\ \text{mm}$  with repeatability in x-axis of  $5\ \mu\text{m}$  and the in z-axis  $1\ \mu\text{m}$ . By moving the sensor over the sample surface and combining all the profiles measured, a three-dimensional dataset of the investigated surface is created. The sensor is driven over the sample surface by a linear axis.

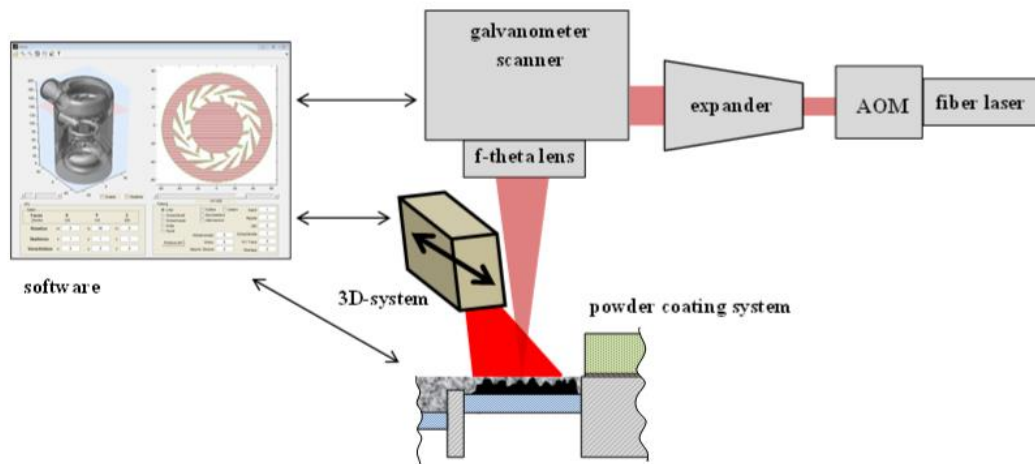


Fig. 2: Schematic set-up for the with in-situ measurement methods for process controlling of high-rate laser microsintering

### **Concept of novel coating system of micro powder**

An ideal coating system for the LMS should fulfill the requirements for achieving dense, homogeneous, reproducible and thin powder layers of thickness under  $20\ \mu\text{m}$  in short time. For this purpose, various coating systems and regimes have already been tested at the LHM. Based on earlier investigation on powder compaction [1, 2], a promising approach to the realization of a closed and condensed powder coat was found, which is shown schematically in Fig. 3. The powder has to be transported from a powder reservoir to the adjacent build platform and simultaneously compacted. Concurrently, the property of the powder to fill existing cavities under pressure is used. By adhesive and friction forces between the powder and the counter plate, the powder transport can also be favored. To maintain the compaction during the coating process, the powder and build platform remain closed by a lid. To counteract the increasing pressure, a higher back pressure has to be put on the lid. The movement of the lid proceeds continuously during the coating process up to releasing the platforms for the irradiation. To avoid losses of the powder during the coating, the applied pressure in the powder reservoir has to be discharged just before releasing the platforms through the lid. In addition, stripper elements next to the platforms should hold the powder back. To generate a sintered body, the sample platform was delivery corresponding to the selected layer thickness after the irradiation and the coating process starts from the beginning.

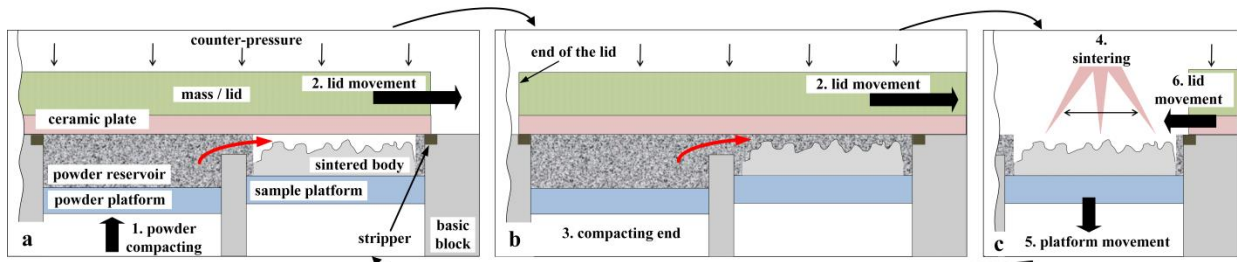


Fig. 3: Schematic and approach of the powder compacting and coating unit. (a) Lid closes powder and sample platform; powder compacting and lid movement at the same time. (b) Lid movement and powder flow to sample direction; before release of the powder reservoir, the compacting ends; lid movement to end position. (c) Opening the sample platform; sintering; delivery of the sample axes. repeating step a to c until the part have been complete

Before the novel coating system was implemented, first the relative change in density of powders under external force should have been examined more closely. Based on the results, an appropriate pressure range for the novel coating system should have been determined. To point out the difference between the commercial sintering and the special features of microsintering, one poor and good flowing metal powder were chosen [Tab. 1].

powder	particle form	particle size $d_{50}$ (num.) / variance	rel. bulk density	atomization
molybdenum	spherical	1.42 $\mu\text{m}$ / +0.7 -8 $\mu\text{m}$	20.3%	gas
tungsten	spherical	14.27 $\mu\text{m}$ / +7 -45 $\mu\text{m}$	53.4%	gas

Tab. 1: Properties of molybdenum and tungsten powder

The reason for the poor coating properties of micro powders (in this case molybdenum powder) is the particle size. Due to the high number of contact surfaces, the adhesive forces among the particles increase rapidly in comparison with the weight force, leading to format agglomerates [6]. This provides for a large number of cavities and thus too low bulk density, which will result in low sinter density. In addition, the flowability of the powder is significantly reduced. In Fig. 4a, the agglomerates in the molybdenum powder are clearly visible.

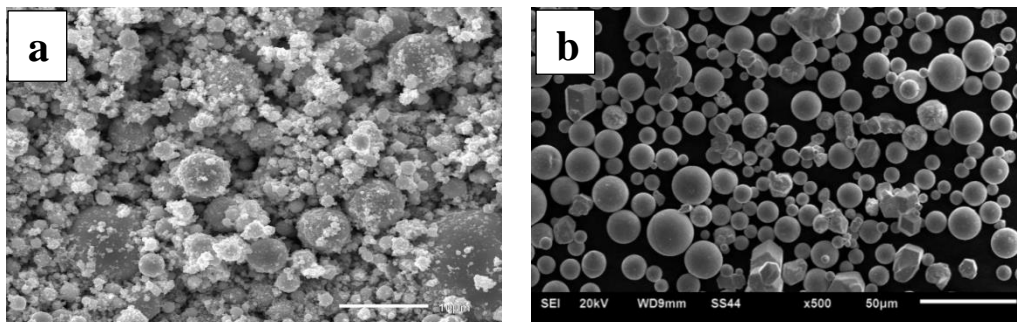


Fig. 4: SEM micrographs presenting metal powders of different particle size. (a) Micro molybdenum powder with agglomerate and poor flow properties. (b) Macro tungsten powder providing good flow properties. Both powders are gas atomized.

The Investigations for powder compaction shown that a high relative density change up to 60% was achieved for molybdenum powder. For the tungsten powders, however, the density change was only 3% [Fig 5]. Due to the good flowability of the tungsten powder, high packing densities were reached in the inactive state. The high density increase for

molybdenum powder is caused by many cavities present in the powder, as previously explained.

Especially at the beginning of the pressure increase, the change in density is the highest. Thus, a lot of agglomerates are destroyed and the numerous existing cavities closed. The current coating system is to be classified in this pressure range. The high density changes in this range are one reason for the poor coating properties. When the pressure is further increased, first the density change is reduced and the number of contact surfaces and thus the cohesive forces increase strongly. After that, the rise in pressure causes the elastic and plastic deformations. The results show that especially in molybdenum powders the compaction is advantageous, which can also be confirmed by previous investigations to increase the packing density [1, 2].

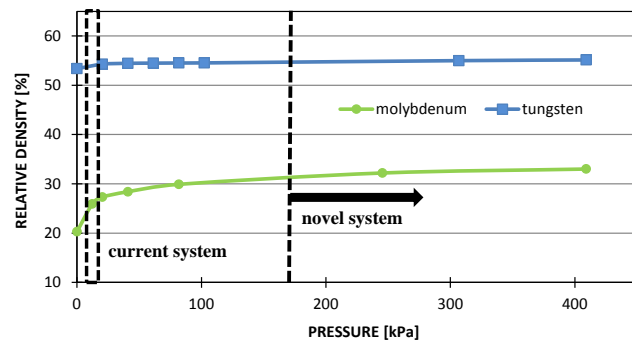


Fig. 5: Powder compacting, relative density vs. pressure for molybdenum powder ( $d_{50}=1.42 \mu\text{m}$ ) and tungsten powder ( $d_{50}=14.27 \mu\text{m}$ )

Based on the results, a novel coating system was implemented and is illustrated in Fig. 6. Related to the results from the powder compaction a minimal pressure of 150 kPa was chosen. From this value, the relative density increases only slightly. To build up the pressure in the powder reservoir and maintain it during the coating process, adjustable pressure springs were attached to the lid. The high pressure may cause increased adhesive and friction forces and high torque impact. To counteract these effects, the lid moves on sliding elements and is supported by lateral guide rails. Therefore a uniform movement of the lid can be guaranteed. For the linear movement of the lid from the present electric drive (current coating system) is converted to high-performance piston cylinder. Also the compaction of the powder takes place with a piston cylinder. This makes it possible to fast implement a defined and high power. However, an exact delivery is required for the movement of the sample axis and therefore a stepping motor is continue used. As a counter plate for powder reservoir a ceramic was chosen, as well as on the current coating system, where ceramic proved itself to be a counter-partner to the powder due to high wear resistance.

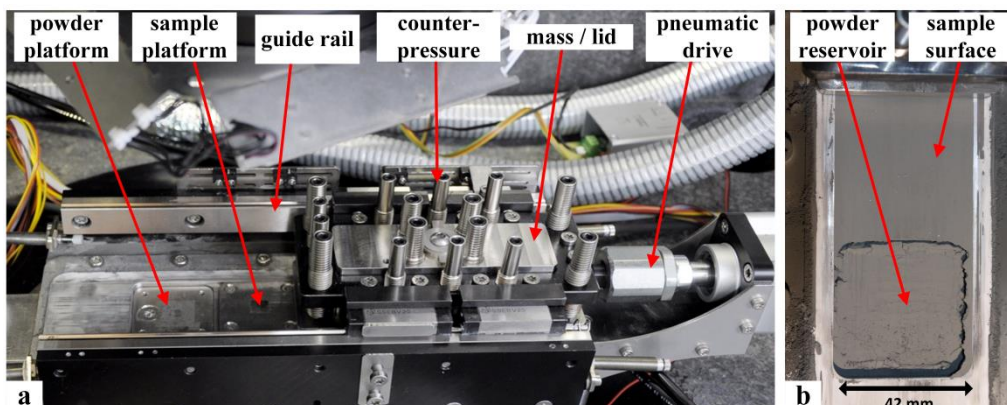
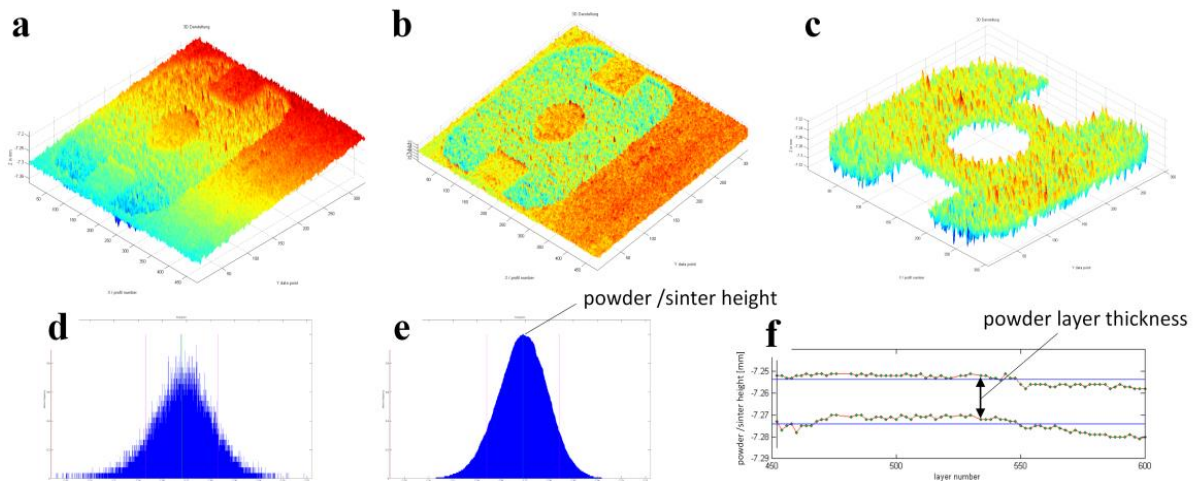


Fig. 6: (a) Novel powder coating device; under the powder platform is a pneumatic cylinder for powder compacting; sample platform is moved by a stepper motor; the counter pressure is effected by pressure springs; the lid movement is realized with a pneumatic piston rod cylinder; the guide rail, take the resulting forces on. (b) top view of a first promising attempt for powder coating with micro molybdenum powder.

### 3D-measurement of an sintering process with the novel coating system

During the sintering process, the powder and sinter height are measured and documented to assess the coating system. On the basis of the topography images obtained, the powder and sinter height was determined and the corresponding standard deviation was calculated. These values were graphically analysed over the full building process.

A typically procedure of the analyzing process from a sintered specimen is shown in Fig. 7. To obtain suitable measurement values, the topography images are recomputed using the software Matlab. Therefore, the tilting between the measurement axis and the sample surface was a problem. For this purpose a tilt correction of the topography images was integrated in the analysis, which was done once in advance. Another problem was the areas outside the sintered body because only the sintered part is relevant for the analysis of the powder and sinter layers. Due to this, a target contour superposition was added to the analyzing process. To achieve this, a defined ablation structure were captured and measured with the 3D sensor, also done in advance. With this it was possible to determine the center of the scanning field and the resolution of the 3D sensor and a superposition could be done. After these adjustments, the distribution (histogram) of the measured height of the sintered structure was determined and from this the most frequent value was chosen as average powder or sinter height. Furthermore the standard deviation (SD) of the distribution was calculated. To obtain the exact height value, the measured 3D profile was interpolated in order to smooth measurement errors caused by measurement inaccuracies, signal noise and partially signal shadowing. The mentioned post processing were done with each measured layer. Finally, the powder layer thickness was calculated from the height difference of the powder and sinter body surface.



*Fig. 7: Evaluation of a sintered surface with the 3D measurement system: (a) raw data of the measurement. (b) Tilt correction and scan field adjustment. (c) Target contour overlay. (d) Histogram of non-filtered data. (e) Histogram of filtered data, maximum frequency is the powder or sinter height. (f) powder and sinter height changes with increasing layer numbers*

Inhomogeneities and surface defects of either the powder or sinter layer or both can be detected by taking into account the standard deviation (SD). This is demonstrated in Fig. 8 showing the measurement data of two different powder layers. In Fig. 8a, a Gaussian distribution of the height values can be observed indicating a homogeneously dispensed powder layer, with a low SD, Fig. 8 (a, b). On the other hand, a inhomogeneous distributed powder layer is shown in Fig 8 (c, d). This powder layer defect can be detected by the a

significant higher SD of the measured 3D profile. However, to identify the minimal SD for a given powder layer, a reference measurement was carried out using a compressed powder bed. The minimal SD for this ideal powder layer was  $5.3\ \mu\text{m}$  or  $12\ \mu\text{m}$ , obtained for molybdenum and for tungsten, respectively. These SD values obtained are in the range of the particle size of the used powder. Due to the difference of the SD, the deposited powder layers can be described and analyzed quantitative.

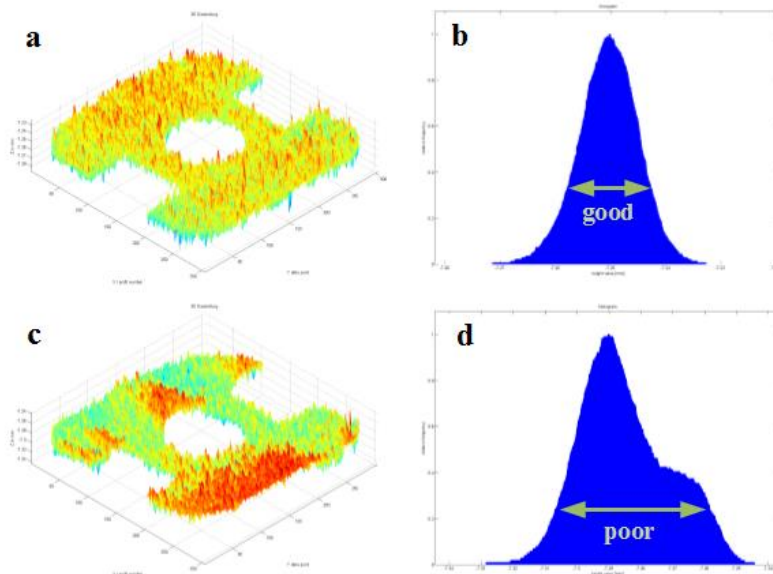


*Fig.8: Topography images and histogram of a good (a, b) and a poor (c, d) powder layer. standard deviation: (b)  $SD=6\ \mu\text{m}$  (d)  $SD=9.7\ \mu\text{m}$*

Fig. 10 shows the height of the powder layer (molybdenum) as measured during the sintering process with progressive layer number. For the sintering of the specimen suitable parameters from previous experiments were used. To investigate the correlation between the measured data and process variations, experimental parameters, for example laser power, powder and sinter layer thickness, have been varied during the sintering process. In the areas with unchanged parameters an average powder layer of  $18\ \mu\text{m}$  and a SD of  $7\ \mu\text{m}$  were observed. Due to a second movement of the lid over the sample platform, without adding further powder and without sintering, the powder layer thickness could be reduced to  $13\ \mu\text{m}$  and the SD to  $6\ \mu\text{m}$ . The low variances to the ideal SD and the low powder layer thickness from less than  $20\ \mu\text{m}$  show the functionality of the novel coating system. These thin, homogeny and reproducible powder layers were produced with 1.5 seconds powder coating times. This is about 4 times faster than powder coating using the current coating system.

From the results obtained in laser sintering using varied processing parameters, the following correlation can be derived: As a first, with lower laser power (reduced from 50% to 40%) the powder layer thickness increased that will enlarge the variations of the sinter layer thickness. As a result, the degree of melting and thus the sinter density will potentially decrease, as can be seen in Fig. 10a. The increase of the laser power up to 60%, by contrast, a significant reduction of the fluctuation of the powder and sinter height was detected. From this, it can be suggested that an optimal laser power for a given sinter layer thickness has to be chosen. A further increase of the laser power (70%) resulted in powder vaporization due to

the higher intensity in the beginning of the sintering till a suitable powder layer thickness is reached. Furthermore the surface roughness increases due to increase of the fluctuation of the sinter layer thickness. This variation of the laser power can be recognized in the cross section of the specimen through the surface density given in Fig. 9.

Furthermore, the impact of a too small axis step (lower sinter layer thickness) without adaption of other process parameters was studied. The smaller axis step reduced the distance between the sinter surface and the lid of the coating system. This results in an inhomogeneous and disturbed powder layer, which can be detected by the increase of the SD in the powder layer, as discussed above. Due to this, countermeasures in a timely could be taken and a grinding or canting could be avoided. In addition, an fragmentary powder layer was purposely generated, which can occur as a result of changing powder properties, i.e. moisture content, production error, etc., that will detrimentally affect the coating properties. It can be seen, that a missing powder layer can be detected in the measurement of the powder and sinter height as well as in the SD. With this it is possible to take countermeasures rapidly.

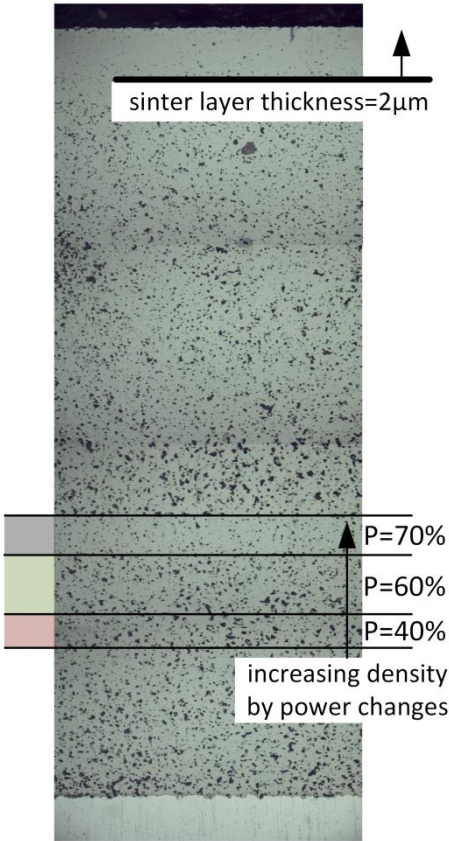


Fig. 9: Cross section of the sintered specimen, bottom: increasing density by power change; on top: high density by sinter layer thickness of 2  $\mu\text{m}$  (without 3D-measurement).

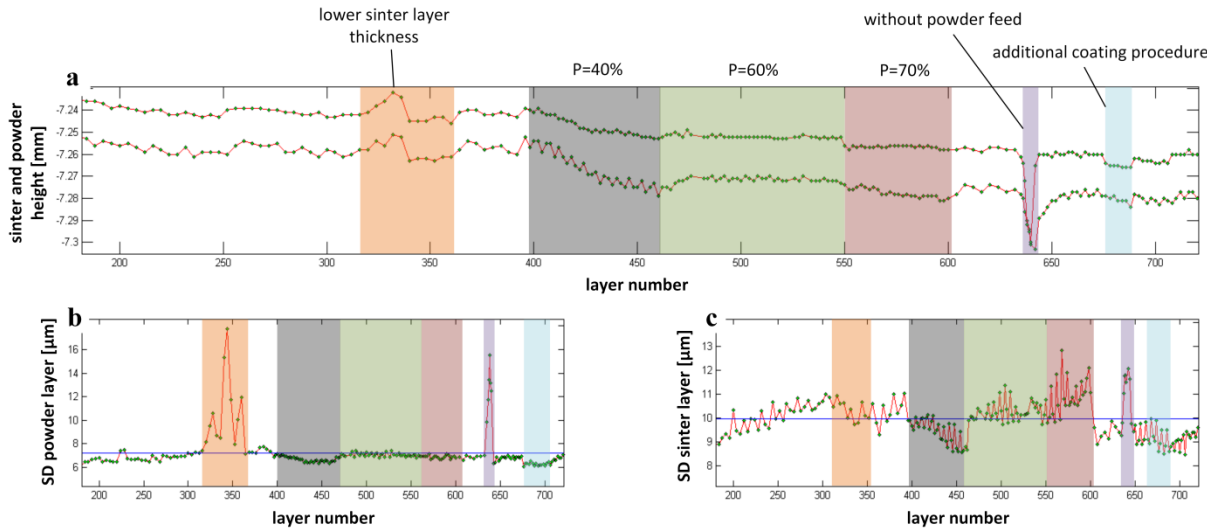
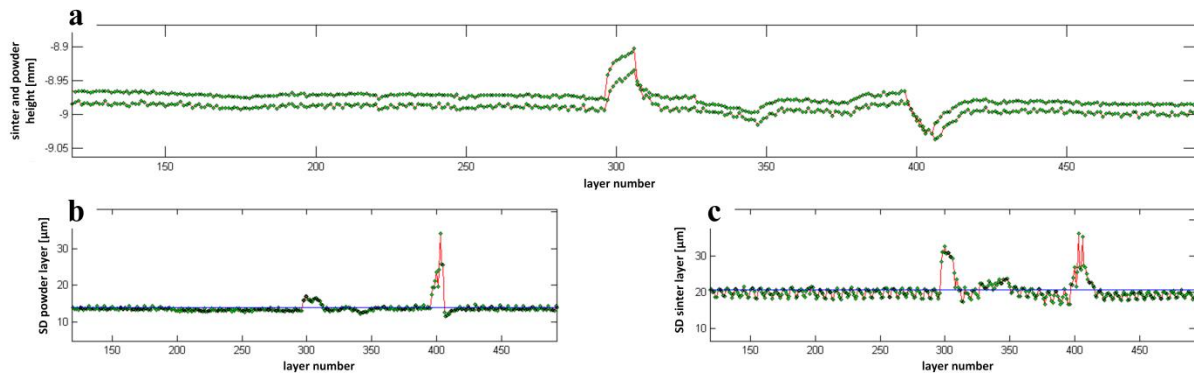


Fig.10: 3D measurement of a building process with molybdenum powder; the color section shows the area of parameter changes. (a) Powder and sinter height variation with increasing layer numbers. (b) Standard deviation of the powder layers. (c) Standard deviation of the sinter layers. (P is laser output power)

In addition to the previous study, laser sintering of tungsten powder was investigated with regards to powder and sinter layer thickness as well as homogeneity, Fig. 11. For the measurement shown a axis step of 6  $\mu\text{m}$  (sinter layer thickness) was chosen. The 3d analysis of the powder layer yielded an average powder layer thickness of 17  $\mu\text{m}$ , the standard deviation was 14  $\mu\text{m}$ . In Fig. 11 it can be seen that the powder coating remained very stable during the coating process that is due to the good flow properties of the tungsten powder. By varying the laser or coating parameters, however, strong variances of both powder height and SD were detected that can be seen for the layer numbers ranging from 280 to 420.



*Fig.11: 3D measurement of a building process with tungsten powder: (a) Powder and sinter height variation with increasing layer numbers. (b) Standard deviation of the powder layers. (c) Standard deviation of the sinter layers. At layer number 280 was increased the powder thickness; between the layer numbers 320 and 380 was varied the laser power; between the layer numbers 380 and 420 missing the powder layer.*

### Proof of concept by first sinter results

First investigations with the novel coating system for the generation and optimization of different test structures have already been performed. Fig. 12 shows a selection of the test structures using the CW-high power laser and a fast beam deflection as shown in Fig. 2. The results were very promising and show that with the novel coating regime sintered body's with density up to 95% and steep overhangs up to 75% can be achieved. Due to the compacted powder bed around the sinter body no support structures for the overhangs were required. In addition, wall thickness of 40  $\mu\text{m}$  was obtained. The sintered layer thickness minimally achieved was 2  $\mu\text{m}$  with build speed up to 300  $\text{mm}^3/\text{h}$ .

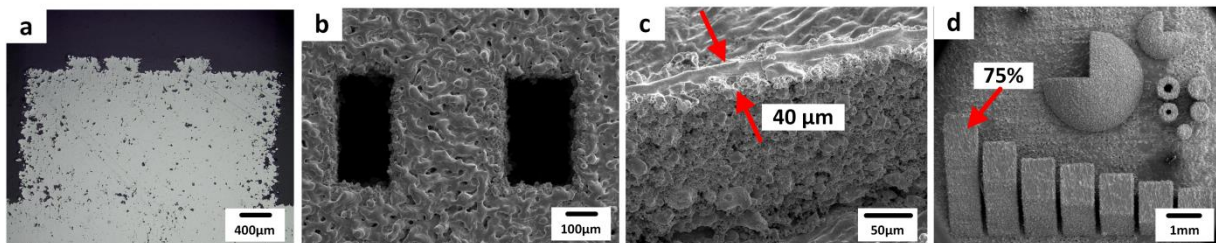


*Fig.12: (a) Cross section through a sintered specimen with density of around 95%. (b) SEM picture of sintered surface. (c) SEM picture of a wall with 40  $\mu\text{m}$  thickness. (d) SEM picture of test structures with overhang up to 75%.*

## Summary and Outlook

Laser microsintering is constantly subject to further development at the LHM to improve the productivity, sinter quality and the reproducibility of the process. Therefore, a field of development focuses on the optimization of the powder coating with regard to powder compaction, coating speed and homogeneity. For this purpose, a novel coating concept was developed and built up. With an integrated in-situ 3D measurement method, the generation of homogeneous and thin powder layers has been proven. Based on high sinter densities of the specimens, achieving of high packing density of powder can be proven. The evaluation of the measurement results of the 3D system also show that there are also possibilities for process optimization and the detection of building errors. Due to the potential for error detection, a direct process control should be integrated to improve the reproducibility of the process, in the future. To detect errors which produce no difference in height, such as oxidation or deviations of the degree of melting, a camera system for detection of contrast differences is to be additionally integrated. For this purpose, first developments are already in progress at LHM. A further development of the presented coating system with two powder reservoirs is being prepared. This should provide further shortening of the coating time.

## Acknowledgements

The authors gratefully acknowledge financial support of the present work by the Federal Ministry of Education and Research (FKZ: 8230135), the European Union and the Free State of Saxony.

## References

- [1] A. Streek, P. Regenfass, R. Ebert, H. Exner: *Laser micro sintering – a quality leap through improvement of powder packing*. In: D. L. Bourell et al. (Eds): *The Proceedings of the 19th Annual SFF Symposium 2008*, 297-308.
- [2] A. Streek, P. Regenfass, R. Ebert, H. Exner: *Laser micro sintering - upgrade of the technology*. ICALEO 2009–28th International Congress on Applications of Lasers and Electro-Optics, Congress Proceedings, Orlando, FL, USA, Volume: 102
- [3] A. Streek, P. Regenfass, C. Schulze, H. Exner: *High Resolution Laser Melting with Brilliant Radiation*. *The Proceedings of the 25th Annual SFF Symposium 2014*
- [4] A. Streek, M. Horn, M. Erler, L. Hartwig, U. Löschner, H. Exner: *3D Microprint von Metallen mit Laserstrahlung – verfügbare Technologien*. *Laser in der Elektronikproduktion & Feinwerktechnik, Tagungsband: LEF 2014*
- [5] Franka Marquardt, Bernhard Steiger, Dana Quellmalz: *Schnelle Laserstrahlschaltung - Welchen Beitrag liefern akustooptische Modulatoren für das effiziente und schnelle Schalten von Laserstrahlung?* *Optik & Photonik*, Volume 8, Issue 3, pages 64–67, September 2013.
- [6] D. Schulze: *Pulver und Schüttgüter*. 1. Auflage, Springer-Verlag Berlin Heidelberg, 2006